Fast IPSCs in rat thalamic reticular nucleus require the $GABA_A$ receptor β_1 subunit

Molly M. Huntsman and John R. Huguenard

Department of Neurology and Neurological Sciences, Stanford University Medical Center, Stanford, CA 94305, USA

Synchrony within the thalamocortical system is regulated in part by intranuclear synaptic inhibition within the reticular nucleus (RTN). Inhibitory postsynaptic currents (IPSCs) in RTN neurons are largely characterized by slow decay kinetics that result in powerful and prolonged suppression of spikes. Here we show that some individual RTN neurons are characterized by highly variable mixtures of fast, slow and mixed IPSCs. Heterogeneity arose largely through differences in the contribution of an initial decay component ($\tau_D \sim 10$ ms) which was insensitive to loreclezole, suggesting involvement of the $GABA_A$ receptor β_1 subunit. Single-cell RT-PCR revealed the presence of β_1 subunit mRNA only in those neurons whose IPSCs were dominated by a rapid and prominent initial decay phase. These data show that brief, β_1-dependent, loreclezole-insensitive IPSCs are present in a subpopulation of RTN neurons, and suggest that striking differences in IPSC heterogeneity within single neurons can result from of the presence or absence of a single $GABA_A$ receptor subunit.

(Resubmitted 31 January 2006; accepted after revision 6 February 2006; first published online 9 February 2006)
Corresponding author J. R. Huguenard: Department of Neurology and Neurological Sciences, Room M016, Stanford University, Stanford University Medical Center, Stanford, CA 94305-5300, USA. Email: john.huguenard@stanford.edu

The neurons in the thalamic reticular nucleus (RTN) are GABAergic and are the primary source of inhibition to relay nuclei in the dorsal thalamus and to each other through axon collaterals (Scheibel & Scheibel, 1966; Houser *et al.* 1980; Yen *et al.* 1985; Cox *et al.* 1996; Pinault *et al.* 1997). Mutual connections within the RTN provide a powerful source of intranuclear lateral inhibition mediated through slowly decaying $GABA_A$ receptor-mediated IPSCs (Ulrich & Huguenard, 1997; Zhang *et al.* 1997). Focal blockade of $GABA_A$ receptors results in disinhibition within the RTN, yielding a higher inhibitory output onto thalamic relay neurons (Huguenard & Prince, 1994; Sanchez-Vives & McCormick, 1997; Sanchez-Vives *et al.* 1997). IPSCs in the RTN are critically important in regulating intrathalamic synchrony, as demonstrated in various rodent models. For example, in mice with an inactivated $GABA_A$ receptor β_3 subunit gene the recorded IPSCs in RTN neurons are brief and small, and oscillatory network activity in the thalamus becomes hypersynchronous (Huntsman *et al.* 1999), such that it resembles that observed in animal models of absence epilepsy (Inoue *et al.* 1993). By contrast, benzodiazepine application results in prolonged RTN IPSCs (Browne *et al.* 2001), and a suppression of thalamic oscillations (Huguenard & Prince, 1994). Computer simulations have shown that IPSC decay kinetics in RTN neurons play a key role in determining the duration of thalamic synchronous activity (Sohal *et al.* 2000).

The slow decay kinetics of spontaneous IPSCs (IPSCs) in prototypical RTN neurons are unique compared to those observed in many other neuronal types. The weighted decay time constant ($\tau_{D,W} > 60$ ms at 23°C) is three times slower than IPSCs in neighbouring relay nuclei of the thalamus (Zhang *et al.* 1997; Huntsman & Huguenard, 2000; Okada *et al.* 2000) as well as other brain regions (~10–25 ms; Galarreta & Hestrin, 1997; Xiang *et al.* 1998; Vicini *et al.* 2001). Many factors may contribute to variations in IPSC decay kinetics, but the major determinant is likely to be cell-specific expression of different $GABA_A$ receptor subunits. During spontaneous synaptic events, where GABA concentration in the synaptic cleft is high and probably favours high occupancy (Maconochie *et al.* 1994; Jones & Westbrook, 1995), and reuptake mechanisms are not a major factor (Draguhn & Heinemann, 1996), then time course is mostly dependent upon the stochastic properties of the postsynaptic receptors (Jones & Westbrook, 1995; Jones *et al.* 1998). While secondary factors, such as post-translational changes, can influence $GABA_A$ receptor function (Jones & Westbrook, 1997; Poisbeau *et al.* 1999), there is evidence that the expression of individual $GABA_A$ receptor subunits is a primary regulator of decay rate for GABA-gated chloride channels (Gingrich *et al.* 1995; Jones & Westbrook, 1995). The two primary $GABA_A$ receptor subunits expressed in RTN (α_3 and β_3), when coexpressed with other subunits, have been reported to show some of

 DOI: 10.1113/jphysiol.2006.106617

the slowest desensitization rates (Verdoorn, 1994; Gingrich *et al.* 1995; Burgard *et al.* 1996).

Heterogeneity of synaptic inhibition in hippocampal or cortical neurons (Banks *et al.* 1998; Hefti & Smith, 2000; Garden *et al.* 2002; Xiang *et al.* 1998; Kobayashi & Buckmaster, 2003) is expected based on the expression of supernumerary receptor subunits in these regions. For example, all of the major subunits (except the α_6 subunit, which is restricted to cerebellar neurons) are expressed in hippocampal CA1 and CA3 cells (Wisden *et al.* 1992). Binding of various allosteric modulators, such as benzodiazepines, barbiturates, anticonvulsants and neurosteroids (all of which mainly prolong IPSC duration), is dependent on the specific subunit composition of the receptor (MacDonald & Olsen, 1994). The different clinical actions of these drugs, ranging from myorelaxant to anticonvulsant, anxiolytic and sedative, illustrate the importance and complexity of IPSC regulation in different brain regions.

The functional diversity of GABAergic synaptic inputs in each region should logically be related to the number of locally expressed receptor subunits. Yet the subunit distribution in the RTN predicts minimal functional diversity. Only four of the 19 existing subunits (α_3, β_1, β_3 and γ_2) are present above background levels in RTN (Wisden *et al.* 1992; Fritschy & Möhler, 1995; Huntsman *et al.* 1996; Pirker *et al.* 2000). Therefore, $GABA_A$ receptors in RTN neurons are likely to be limited to a few subtypes. Here we show that despite this limited $GABA_A$ subunit heterogeneity in RTN, IPSC decay is not uniform. In single RTN cell recordings, we found IPSCs with both slow and fast decay rates, and that the relative numbers of fast and slow IPSCs varied on a cell to cell basis. In an attempt to elucidate the molecular basis of this heterogeneity, we examined the effects of two compounds that target specific $GABA_A$ receptor subtypes in the RTN: the benzodiazepine clonazepam (whose activity depends on $\alpha_{1,2,3,5}$ and γ_2 subunits; Pritchett *et al.* 1989), and loreclezole (which depends on β_2 or β_3 subunits; Wafford *et al.* 1994; Wingrove *et al.* 1994). We then combined the information gained from electrophysiology with single-cell RT-PCR experiments to correlate these unique functional properties with $GABA_A$ receptor subunit expression. We found that functional heterogeneity is not only present in the RTN, but that it is likely to be determined by the presence or absence of a single subunit (β_1). A preliminary report of this work has been presented (Huntsman & Huguenard, 2001).

Methods

Preparation of thalamic slices

All experiments were performed in accordance with National Institutes of Health *Guide for the Care and Use of Laboratory Animals* and were approved by the Stanford University Institutional Animal Care and Use Committee. Thalamic slices were obtained from Sprague-Dawley rats (of either sex) ranging in age from postnatal day 21 (P21) – P30. Animals were fully anaesthetized (50 mg kg^{-1} sodium pentobarbital, administered I.P.) before decapitation and brains were blocked and removed from the skull. The blocked brain was then placed in ice-cold, oxygen equilibrated (95% O_2–5% CO_2) sucrose slicing solution for 2–3 min (mM): 234 sucrose, 11 glucose, 24 $NaHCO_3$, 2.5 KCl, 1.25 $NaH_2PO_4.H_2O$, 10 $MgSO_4$ and 0.5 $CaCl_2$. The brain was glued to a slicing dish, ventral surface down, and submerged in cold sucrose slicing solution. Horizontal slices that included the dorsal thalamus and adjacent reticular nucleus were cut at a 200-μm thickness with a vibrating blade microtome (Leica). Slices were then incubated in preheated (32°C), oxygen equilibrated standard artificial cerebral spinal fluid (ACSF) (mM): 126 NaCl, 26 $NaHCO_3$, 10 glucose, 2.5 KCl, 1.25 $NaH_2PO_4.H_2O$, 2 $MgCl_2.6H_2O$ and 2 $CaCl_2.2H_2O$ for at least 1 h prior to recording.

Electrophysiology

Whole-cell patch-clamp recordings were obtained by previously published methods (Huntsman & Huguenard, 2000). Briefly, after a 1 h incubation period, sections were transferred to a chamber and bathed in a continuous perfusion of ACSF (2 ml min^{-1}) at room temperature (~24°C). Whole-cell patch-clamp recordings were made from visually identified neurons within the boundaries of the reticular nucleus. The recordings were made under visual control using a fixed-stage upright microscope (Axioskop, Zeiss, Thornwood, NY, USA) equipped with an insulated 63× objective, Nomarski optics and an infrared-sensitive video camera (Cohu, Inc., San Diego, CA, USA). The internal pipette solution contained (mM): 135 CsCl, 5 lidocaine *N*-ethyl bromide (QX-314), 2 $MgCl_2$, 10 ethyleneglycol-bis(β-aminoethyl ether)-*N*,*N*,*N*′,*N*′-tetraacetate acid (EGTA) (Sigma, St Louis, MO, USA), and 10 *N*-2-hydroxyethylpiperazine-*N*′-2-ethanesulphonic acid (Hepes) (Sigma). The solution was adjusted with CsOH to pH 7.3; final osmolarity was 290 mosmol l^{-1}. Glass electrodes (borosilicate glass, Garner Glass Company, Claremont, CA, USA) were pulled in multiple stages using a Flaming-Brown micropipette puller (Model P-87, Sutter Instrument Co., Novato, CA, USA). Pipettes had resistances of 2.5–3.3 MΩ when filled with intracellular pipette solution. Continuous voltage-clamp records containing spontaneous IPSCs were obtained at a holding potential of −60 mV using a patch clamp amplifier (model L/M-EPC 7, List Medical, Darmstadt, Germany) or a Multiclamp amplifier (700A, Axon Instruments, Union City, CA, USA). Series resistance was always less

than 15 MΩ and monitored throughout the experiment for stability (< 25% change), and was not electronically compensated.

$GABA_A$ receptor-mediated spontaneous IPSCs were pharmacologically isolated by bath application of the ionotropic excitatory amino acid receptor blockers: 6,7-dinitro-quinoxaline-2,3-dione (DNQX, 20 μm, Sigma-RBI, Natick, MA, USA) and 2-amino-5-phosphonopentanoic acid (AP-5, 100 μm, Sigma-RBI) in physiological saline. The perfusion rate was 2 ml min^{-1} and it typically took 2–3 min to fully block all excitatory synaptic responses. $GABA_B$ receptors were blocked with 135 mM Cs^+ and 5 mM QX-314 in the internal pipette solution. GABA modulators clonazepam (Sigma-RBI) and loreclezole (a gift from Janssen Research, Belgium) were dissolved at 1000× final concentration in DMSO and frozen in aliquots. Vehicle controls contained equivalent final DMSO concentration (0.1%). Fresh dilutions of the concentrated stocks were made daily and applied by bath perfusion. As slow wash-in times (> 10 min, Fig. 2) impeded the quantification of equilibrium drug effects, we mainly examined cells after preincubating (cf. Hollrigel *et al.* 1996) for 1–2 h in clonazepam (100 nM) or loreclezole (10 μM). In order to examine action potential-independent mini IPSCs (mIPSCs), we recorded sIPSCs in the presence of 1 μM TTX (Sigma). TTX did not affect frequency of events, indicating that the vast majority of sIPSCs in our preparation were mIPSCs.

Single-cell RT-PCR

Analysis of β_1 subunit mRNA expression was achieved by single-cell RT-PCR. Methods followed similar single-cell RT-PCR guidelines previously described (D. K. O'Dowd, personal communication; Monyer & Jonas, 1995; Massengill *et al.* 1997; Berger *et al.* 1998; van Hooft *et al.* 2000). Gloves were worn at all times and all solutions were autoclaved prior to use. The silver wire electrode was re-chloridized with bleach prior to each day of recording. The cytoplasm of each RTN neuron was aspirated into the pipette after the whole-cell patch clamp recording was complete (usually 10–15 min total recording time). Electrophysiology was carried out in the same manner as described above with the exception that pipettes were pulled to a resistance in the range of 1.8–2.5 MΩ. RT-PCR was always performed on the same day of whole-cell patch-clamp recording in order to avoid any freeze–thaw irregularities. Cell cytoplasm was harvested by applying negative pressure to the recording pipette under visual control and expelled into an autoclaved tube containing 1 mM deoxynucleoside 5′-triphosphate mixture and 100 ng μl^{-1} random primers. Each cell's contents were placed on ice until the last cell was harvested and then all were processed together. Controls were nuclease-free water, intracellular pipette solution (a pipette filled with intracellular solution and held above a thalamic slice under flowing ACSF for a few minutes) and 40 pg of total RNA isolated from rodent thalamus were included in every reverse transcription reaction set. The solution was brought to a volume of 10 μl with nuclease-free water, incubated at 65°C for 10 min and put on ice. All reactions were added to new autoclaved tubes containing: 1 × First-strand transcription buffer, 10 mM dithiothreitol (DTT), 20 units of ribonuclease inhibitor (RNaseOUT; Invitrogen, Carlsbad, CA, USA), and 50 units of Moloney murine leukaemia virus reverse transcriptase (Invitrogen Life Technologies). This mixture was incubated for 50 min at 37°C, then heat inactivated at 70°C for 15 min. The entire cDNA template reaction (10 μl) was used in the first round of PCR amplification. The primer pairs were chosen to amplify the heterogeneous cytoplasmic loop of the β_1 subunit of the $GABA_A$ receptor. The forward primer was 5′-GCA-ATA-TTC-TCC-TCA-GCA-CC-3′ and corresponds to nucleotides 1169–1190 of the rodent sequence (Ymer *et al.* 1989) and the reverse primer was 5′-GTT-CAC-GTC-AGT-CAA-GTC-A-3′ and corresponds to nucleotides 1400–1418. For the second round of PCR, two nested primers (internal to the first round pair) were used. The forward primer was 5′-GAG-GTG-CTC-ACG-GGT-GTA-AG-3′ and corresponded to nucleotides 1221–1240 of the rodent sequence (Ymer *et al.* 1989) and the reverse primer was 5′-CTG-AGA-GGC-ACG-TCT-GCG-GAT-G-3′ and corresponds to nucleotides 1361–1382. The nested primers yielded a single PCR product of 162 bp. The first round PCR reaction was done in a master mix with the total number of reactions being determined by the number of cells collected for the day of recording along with all the controls. In addition to amplifying the three controls from the RT reaction, a water control was also included in the master mix for each round of PCR. In a 50-μl reaction the ingredients were as follows: 1 × PCR buffer, 0.2 mM dNTP mixture (each), 1.5 mM $MgCl_2$, 20 pmol μl^{-1} of the outer primer pair, nuclease free water, the contents of the cDNA template reaction from a single cell (or the contents of cDNA reactions done in the presence of water, pipette solution and total RNA controls) and 2.5 units of DNA polymerase (Platinum *Taq*, Invitrogen Life Technologies). The PCR conditions were as follows: one denaturing step at 94°C for 1 min, 35 cycles of amplification representing 3 steps of denaturing, annealing and extension (94°C for 30 s; 55°C for 30 s; 72°C for 1 min) and a final extension at 72°C for 7 min. After the reaction was complete, 5 μl of the 50 μl total reaction was diluted with 500 μl of RNase free water. Then 5 μl of this dilution was used as the template for the second round of PCR. All reaction and cycling conditions were identical with the exception of the replacement

of the nested (inner) primers. Amplification products were analysed on either a 2% agarose gel or an 8% polyacrylamide gel and always yielded a single ethidium bromide stained-band that migrated at the predicted molecular weight of 162 bp. The molecular weight marker was the pBR322 DNA–*Msp*I digest (New England Biolabs, Ipswich, MA, USA). All products were sequenced at the Stanford University Protein and Nucleic Acid Facility and identified as rodent β_1 cDNA. With two rounds of PCR amplification, false positives were our greatest concern. When a negative control was positive, then the entire round of PCR reactions (and thus entire day of recordings) were eliminated from the study. In some cases DNase I (Promega, Madison, WI, USA) was added prior to RT or RT reactions were run without the enzyme to check for contamination from the nucleus. However, this was not a primary issue because all cell aspirations were done under visual control and uptake of the nucleus could be avoided.

Data collection and analysis

IPSCs were filtered at 1 kHz, stored in digitized form on a Neurocorder (model no. DR484, Neurodata, NY, USA) and backed up on VHS tape. Continuous records of spontaneous events were collected with Axotape v. 2 and Clampex v. 8.2 (Axon Instruments). Spontaneous events were sorted and categorized using the customized software, Detector v. 4.8 (J. R. Huguenard) and Metatape v15.1 (J. R. Huguenard) and analysed with Scan software (courtesy of J. R. Dempster) and Clampfit 8.2 (Axon Instruments). Double exponential fits of baseline-subtracted averaged unitary inhibitory events were made using Clampfit, with DC (offset) forced to zero. The decay of averaged IPSCs was fit to the following equation: $I = A_1 e^{-t/\tau D1} + A_2 e^{-t/\tau D2}$ and weighted time constant $\tau_{D,W} = (\tau_{D1} A_1 + \tau_{D2} A_2)/(A_1 + A_2)$. Data were analysed with Origin v. 6.0 (OriginLab Corp., Northampton, MA, USA) and Microsoft Excel and statistical significance was measured using Student's *t* test. In order to classify RTN neurons into groups based on kinetic properties of sIPSCs an unsupervised hierarchical cluster analysis was used, based on Ward's method, with *z*-score normalization and intervals calculated by Euclidian squared distances (SPSS, v. 12). Following this a multiple discriminant analyis (SPSS), was used to determine which sIPSPC kinetic parameters were most predictive for cluster membership, i.e. those with the highest standardized canonical discriminant function coefficients.

Results

Voltage clamp recordings of $GABA_A$ receptor-mediated spontaneous IPSCs (sIPSCs) were made from a total of 66 neurons in the reticular nucleus (RTN) of the thalamus. All recordings were performed under visual control to identify neurons by position, between external medullary lamina and the internal capsule, and cellular morphology unique to RTN neurons, for example, the fusiform shape of the soma (Jones, 1985). These sIPSCs are for the most part miniature IPSCs (mIPSCs) reflecting spontaneous fusion of GABA containing vesicles. Action potential-dependent IPSCs do not contribute significantly to spontaneous IPSC events in this preparation, as neither the frequency nor the amplitude of sIPSCs was affected by the sodium channel toxin TTX (1 μM, $n = 5$).

IPSCs in RTN neurons are heterogeneous

$GABA_A$ receptor-mediated IPSCs with slow decay times are characteristic inhibitory events in the RTN (Ulrich & Huguenard, 1997; Zhang *et al.* 1997). They are a persistent feature throughout postnatal development on to at least early adulthood (Huntsman & Huguenard, 2000). Although ensemble averages of multiple sIPSCs from single neuron yields mean responses with a slow decay component (Huntsman & Huguenard, 2000), it has been our recent observation that the commonly observed slow IPSCs are interspersed to varying degrees, on a cell to cell basis, with much briefer events. Individual sIPSC duration, as measured by the time required for 90% decay from peak (90%-width), can vary between 10 and 200 ms in a single neuron. This readily ascertained measure (90%-width) provided a simple estimate of IPSC duration that could be ascertained from all individual IPSCs, even from overlapped events, which could not be used for the fitting exponential decay curves.

Figure 1 illustrates IPSC heterogeneity in voltage-clamp recordings from two neighbouring neurons in the RTN. Both neurons possess the distinctive slowly decaying IPSCs (Fig. 1*A* and *B*, open arrowheads). However, the neuron in Fig. 1B has a greater proportion of fast events (Fig. 1*B*, *) intermixed with the characteristic slowly decaying events. In addition, neurons with fast IPSCs often displayed biphasic events – events with both fast and slow decay phases (e.g. Fig. 1*B*, **). Neurons could be roughly classified into two groups based on the kinetics of > 100 ensemble averaged sIPSCs: fast neurons (cells with a fast decay time constant of less than $\sim$18 ms), such as that shown in Fig. 1*B*, had IPSCs with a prominent early rapid decay and slightly larger peak amplitudes. Slow neurons had slower events (Fig. 1*C* and *D*). The degree of heterogeneity varied among RTN neurons and did not appear to reflect any particular location within the RTN. We used unsupervised hierarchical cluster analysis (see Methods) and the kinetic parameters of averaged sIPSCs (A_1, A_2, τ_1, τ_2) to classify individual RTN neurons into two groups. Multiple discriminant analysis was then

used to determine which of the kinetic parameters were most predictive in determining cluster membership. The two time constants, τ_1 and τ_2, were most predictive ($>$ fivefold greater predictive value than either A_1 or A_2) and a discriminant function using only these two parameters $(Z = \tau_1 \times 0.42 + \tau_2 \times 0.021 - 8.94)$ was 100% effective in predicting group membership. Neurons with discriminant function (Z) values < 0.85 were

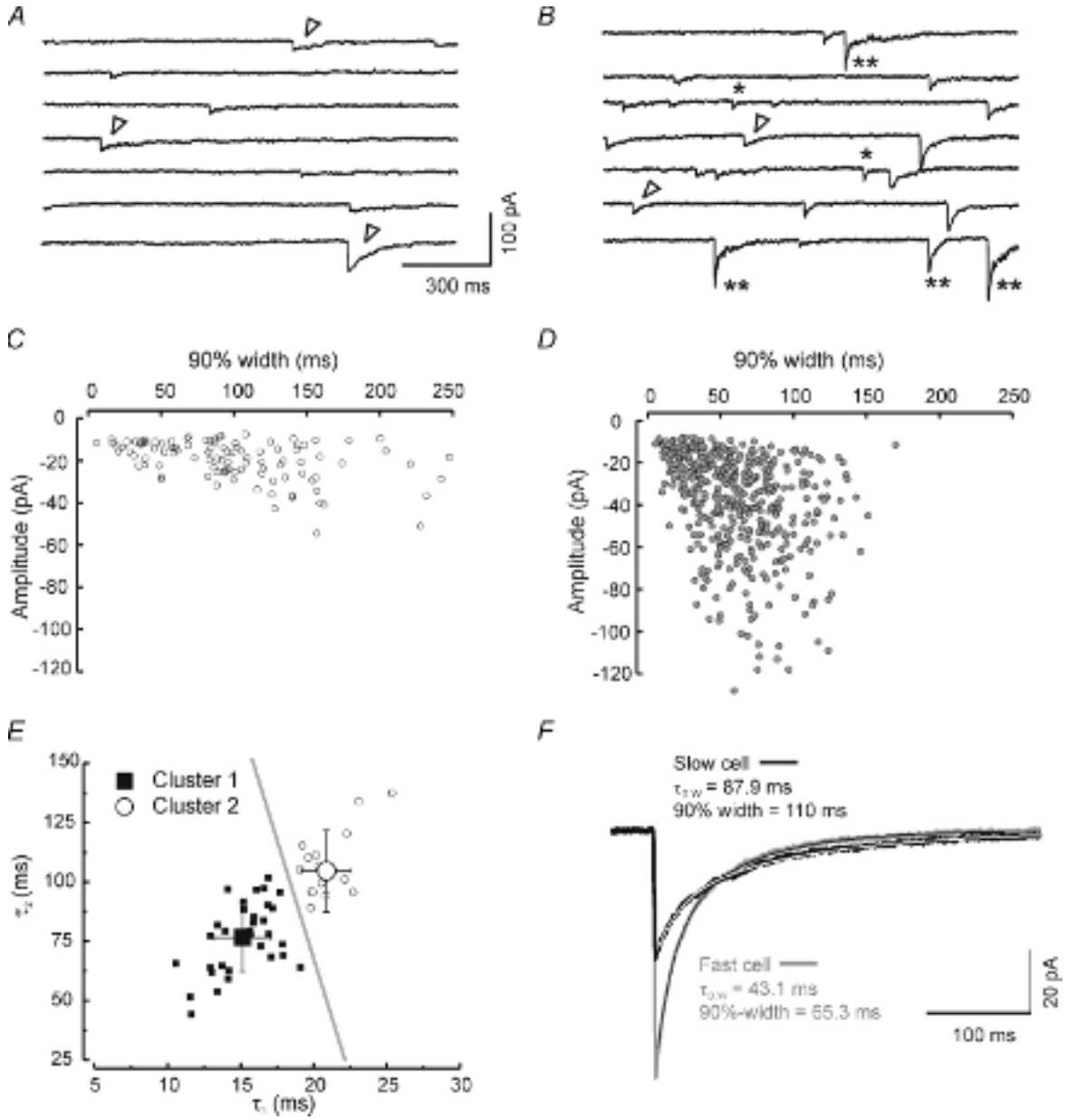

Figure 1. Spontaneous IPSCs from individual RTN neurons have heterogeneous decay properties
Continuous recordings (~10 s) of IPSCs in an RTN neuron dominated by slowly decaying IPSCs (*A*) and a neighbouring neuron in the same microscopic field dominated with fast IPSCs (*B*). Many events have typically slow decay (open arrowheads), while a few individual inhibitory events in the fast cell exhibit simple fast decay (*) or clear biphasic decay (**). *C* and *D*, scatter plots of 90%-widths (the point at which the IPSC has decayed by 90% from its peak) versus peak IPSC amplitude for the same cells represented directly above in *A* and *B*. Each point represents an individual IPSC. Note the cell in *B* and *D* has a majority of IPSCs with fast decays ($<$ 150 ms) and large amplitudes (many events $>$ 60 pA). *E*, scatter plot of late component of decay (τ_2) versus initial component (τ_1) of all control cells ($n = 50$). Unsupervised cluster analysis separates cells into two groups based on τ_1 and τ_2 (see Results). The discriminant function, calculated at the critical Z-score of 0.85, is shown as a grey line. Large symbols indicate mean values and error bars represent standard deviation. *F*, averaged IPSCs superimposed on the same time scale to illustrate differences in peak current amplitude and duration from the slow neuron in *A* and *C* (black trace, $n = 84$ events) and the fast neuron in *B* and *D* (grey trace, $n = 179$ events). The thin dotted lines atop each trace represent double exponential fits.

Table 1. Biexponential decay time constants for ensemble averaged IPSCs for neurons from cluster 1 and cluster 2

	n	A_1 (pA)	A_2 (pA)	τ_1 (ms)	τ_2 (ms)
Cluster 1 (fast)	33	20.24 ± 9.87	14.82 ± 8.41	15.13 ± 1.96	76.6 ± 14.4
Cluster 2 (slow)	17	19.01 ± 12.34	13.52 ± 6.06	20.86 ± 1.71***	104.6 ± 17.1***

Values are means ± S.D. ***Values significantly different between cluster 1 and cluster 2 ($P < 0.0001$).

classified as type I (Fast) and those with values ≥ 0.85 were type II (Slow). When τ_1 is plotted *versus* τ_2 two distinct clusters could be observed (Fig. 1*E*), with τ_1 yielding the less overlapping values than τ_2. Figure 1*E* shows two separate groupings of RTN neurons: those with *Z*-scores < 0.85 were grouped together in the region to the lower left of the grey line in a 'fast' cluster (cluster 1, filled squares) and a second 'slow' cluster (*Z*-scores > 0.5, cluster 2, open circles) with slower τ_1 and to a lesser extent τ_2, values formed another group to the upper right of the grey line. Mean values for IPSC decay time constants and coefficients are shown in Table 1.

In all cases, ensemble-averaged spontaneous RTN IPSCs (obtained with ≥ 100 individual events) were best fitted to two exponentials (Fig. 1*F*). Overall mean values for decay and amplitude from a population of 50 neurons (33 fast + 17 slow) were: $\tau_1 = 17.1 \pm 0.5$ ms, $\tau_2 = 86.1 \pm 2.9$ ms, $A_1 = 19.8 \pm 1.5$ pA, $A_2 = 14.3 \pm 1.1$ pA, and $\tau_{D,W}$ (weighted time constant, see Methods) = 46.03 ± 1.9 ms. The sIPSCs in the example fast cell in Fig. 1 decayed faster in terms of both the fast and slow components ($\tau_1 = 16.4$ ms, $\tau_2 = 72.9$ ms, $\tau_{D,W} = 43.2$ ms) than the slow cell ($\tau_1 = 23.1$ ms, $\tau_2 = 133.0$, $\tau_{D,W} = 87.9$ ms). The biphasic decay observed with ensemble averaged IPSCs (e.g. Fig. 1*F*, fast cell) could be observed in individual IPSCs in some RTN cells (Fig. 1*B*, **).

Heterogeneity of single RTN neuron IPSC kinetics (i.e. the presence of fast and slow IPSCs in the same neuron) persisted in the presence of 2 μM strychnine ($n = 10$, data not shown), indicating that the presence of glycinergic (Ghavanini *et al.* 2005) *versus* GABAergic sIPSCs with different kinetics are not responsible for IPSC heterogeneity that we observe. Bath application of 10 μM bicuculline blocks all synaptic events (both fast and slow, $n = 5$). Taken together, these results show that both fast and slow events are mediated by $GABA_A$ receptors, and suggest that the diverse kinetic responses are mediated by differences in the underlying $GABA_A$ receptors.

We performed a series of experiments ($n = 12$ cells) at more physiological temperatures (34–36°C) in order to determine whether the heterogeneous IPSC kinetics that could be observed within single RTN neurons persisted under these conditions. The kinetics of IPSCs were considerably faster than those obtained at room temperature, consistent with an earlier report (Huntsman & Huguenard, 2000), yet as with room temperature recordings, three types of sIPSCs were observed at higher temperatures, fast events, slow events and hybrid fast–slow events, similar to those shown in Fig. 1*B*.

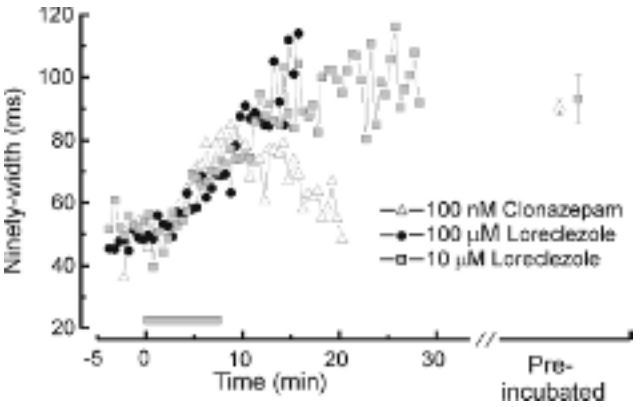

Figure 2. Time course of clonazepam and loreclezole effects on RTN cell IPSCs
Bath application (2 ml min^{-1}) of clonazepam or loreclezole caused significant prolongation of IPSCs during the course of a recording period. IPSC duration was measured by 90%-width, defined as the time required for the IPSC to decay from its peak by 90%. Both drugs have slow wash-in times (8–10 min) and little or no reversibility. The grey bar indicates the time of drug application. Each point represents the mean response of several neurons treated with 100 nM clonazepam ($n = 6$), 10 μM loreclezole ($n = 4$), or 100 μM loreclezole ($n = 10$). The two points to the right of the break on the x-axis indicates the mean values obtained from cells preincubated with either 100 nM clonazepam (mean = 90.4, $n = 11$) or 10 μM loreclezole (mean = 93.2, $n = 14$).

Effects of $GABA_A$ receptor subunit-specific allosteric modulators on IPSCs

In this section we further probe for $GABA_A$ receptor heterogeneity using $GABA_A$ subunit specific allosteric modulators. For these experiments, we used two different methods of drug application: bath application to individual neurons for a defined wash-in time or preincubation of thalamic slices in drug-containing solutions prior to recording. Bath application of either clonazepam (100 nM) or loreclezole (10–100 μM) produced a progressive IPSC prolongation over an extended wash-in period of more than 10 min, and the prolongation was poorly reversible during wash-out (Fig. 2). The effects of loreclezole took much longer to reach peak values than clonazepam and had minimal

reversibility, even during 20 min of wash-out. By contrast, the effects of clonazepam were at least partially reversible during a wash-out period of 10–20 min (Fig. 2).

Pre-incubation of slices in drug-containing solutions (see Methods, also Hollrigel *et al.* 1996) allows for quantification of the equilibrium effects of GABA modulators on IPSCs in the RTN cell population, at the expense of within cell comparisons. Recordings made after a 1-h preincubation with either clonazepam or loreclezole resulted in IPSC durations that were increased above control levels to values similar to, but slightly above, those obtained after 8–10 min of bath application (Fig. 2, on the right of the graph). This result suggests that single cell pharmacology can be reasonably approximated with prolonged bath application and wash-out, but that equilibrium effects can be better assessed by comparing results between slices preincubated for long periods in drug *versus* vehicle containing solutions.

The effects of clonazepam on IPSCs in the RTN

To test whether the two types of IPSCs might arise from synapses with different $GABA_A$ receptor subunits, we examined the effects of the benzodiazepine clonazepam. $GABA_A$ receptors containing the α_3 subunit are modulated to a greater degree than those containing other α subunits (Pritchett *et al.* 1989; Puia *et al.* 1991), and the α_3 subunit is preferentially expressed in the RTN (Huntsman *et al.* 1996). RTN cells exposed to 100 nM clonazepam by either bath application ($n = 6$) or preincubation ($n = 11$) exhibited a significant increase in both the duration and amplitude of IPSCs (Fig. 3). This observation is exemplified in Fig. 3*A–C* for a cell with a 10 min bath application of 100 nM clonazepam. After application of clonazepam, the entire population of IPSCs (both fast and slow events) shifted toward slower events (Fig. 3*B*). Both the fast and slow decay components of ensemble averaged IPSCs were prolonged (Fig. 3*D*; control: $n = 50$ RTN cells, $\tau_1 = 17.1 \pm 0.5$ ms, $\tau_2 = 86.1 \pm 2.9$ ms; clonazepam: $n = 17$, $\tau_1 = 26.3 \pm 1.3$ ms, $P < 0.0001$, $\tau_2 = 134.5 \pm 7.7$ ms, $P < 0.0001$). The average weighted time constant was also significantly increased (e.g. Fig. 3*C*) from 46.0 ± 1.9 ms to 94.5 ± 5.7 ms ($P < 0.0001$). In contrast with the slowing effects of clonazepam on each of the individual time constants of *decay*, only the slowly decaying component was significantly increased in amplitude (Fig. 3*D*; control A_1: 19.8 ± 1.5 pA, $n = 50$, *versus* clonazepam A_1: 23.8 ± 3.1 pA; $n = 17$, $P > 0.2$; control A_2: 14.3 ± 1.1 pA *versus* clonazepam A_2: 39.3 ± 2.8 pA, $P < 0.0001$).

The prolongation of all (both slow and fast) IPSCs by clonazepam suggests that both types of events are mediated by benzodiazepine-sensitive $GABA_A$ receptors, while the selective increase in amplitude of the slowly decaying component suggests that the receptors underlying this part of the IPSC may not be fully saturated by synaptically released GABA (Otis & Mody, 1992; Hájos *et al.* 2000).

The effects of loreclezole on IPSCs in the RTN

In contrast to clonazepam, loreclezole targets regulatory sites on $GABA_A$ receptors composed of β_2 or β_3 subunits (Wafford *et al.* 1994; Wingrove *et al.* 1994). RTN neurons express only β_1 and β_3 subunits but lack β_2 subunits (Huntsman *et al.* 1996; Pirker *et al.* 2000). As with the clonazepam experiments, we examined the effects of loreclezole on IPSCs in RTN by either bath application or preincubation. By contrast with clonazepam, the effects of loreclezole were more selective, producing mainly an increase in IPSC duration, as can be seen from the inset histograms of Fig. 4*A*. Cumulative probability histograms of 90%-width suggested that the slowing of individual IPSCs was largely restricted to events that were initially of long duration – fast events were unchanged (Fig. 4*B*). In ensemble averaged IPSCs, loreclezole selectively prolonged the slow phase of decay while leaving the fast component completely unaffected (Fig. 4*C* and *D*).

Neither fast decay constant (τ_1) nor amplitude (A_1) was altered by loreclezole (Fig. 4*D*, control τ_1: 17.1 ± 0.5 ms, $n = 50$ *versus* loreclezole τ_1: 16.9 ± 1.0 ms, $n = 18$, $P > 0.9$; control A_1: 19.8 ± 1.5 pA, $n = 50$ *versus* loreclezole A_1: 18.7 ± 2.0 pA, $n = 18$, $P > 0.7$). In contrast, the slow time constant of decay (τ_2) was more than doubled by loreclezole (control τ_2: $= 86.1 \pm 2.9$ ms *versus* loreclezole τ_2: 189.5 ± 15.4 ms, $n = 14$, $P < 0.0001$). The amplitude of the slow decay component was also increased by loreclezole (control A_2: 14.4 ± 1.1 pA *versus* loreclezole A_2: 34.1 ± 3.2 pA, $P < 0.0001$). sIPSC weighted time constant ($\tau_{D,W}$) was increased nearly threefold by loreclezole (control $\tau_{D,W}$: 46.0 ± 1.9 ms *versus* loreclezole $\tau_{D,W}$: 130.1 ± 10.7 ms, $P < 0.0001$). In neurons with prominent biphasic individual IPSCs (as in Fig. 1*B*, **), such events were observed even after loreclezole treatment (and in preincubated slices) suggesting that loreclezole selectively enhances the GABA responsiveness at a subpopulation of $GABA_A$ receptors within an individual synapse. To test whether fast decay might be affected by loreclezole in at least a subpopulation of neurons, we made scatter plots of τ_1 *versus* A_1 in individual cells and found instead that the distributions of these two parameters were essentially the same for control and loreclezole (Fig. 5*A* and *B*). This suggests that in no cell was the fast decay process augmented by loreclezole.

Overall, these loreclezole results suggest that fast IPSC decay in RTN cells is mediated by loreclezole-insensitive $GABA_A$ receptors, presumably those lacking either β_2 or β_3 subunits (Wingrove *et al.* 1994; see Discussion).

RTN neurons with fast decay kinetics express β_1 subunit mRNA

In order to determine the molecular basis of IPSC heterogeneity in the RTN, we used single-cell RT-PCR to identify the presence of $GABA_A$ receptor subunit mRNAs. We chose a simple, single message, RT-PCR approach for these experiments, and thus we did not require degenerate primers or compatible multiple primers – reagents that have been used in previous studies utilizing multiplex PCR. Both of these approaches, through competition, reduce primer specificity and the ability to successfully harvest and amplify mRNA from a single cell. The combined message for all ion channel genes is considered to comprise between 0.1 and 1% of the total RNA in a single neuron (Sucher *et al.* 2000). Thus the reduced primer specificity required for multiplex PCR would pose an especially difficult problem for studies of RTN neurons in which $GABA_A$ receptor transcripts in general are extremely low in abundance (Wisden *et al.* 1992; Huntsman *et al.* 1996). While we could not rule out false negatives, we hoped to increase the probability of amplifying β_1 subunit message by using specific primers in two rounds of simplex RT-PCR reactions using nested primers (see Methods).

Examples of two RTN neurons for which we were able to obtain both physiological recordings and single-cell

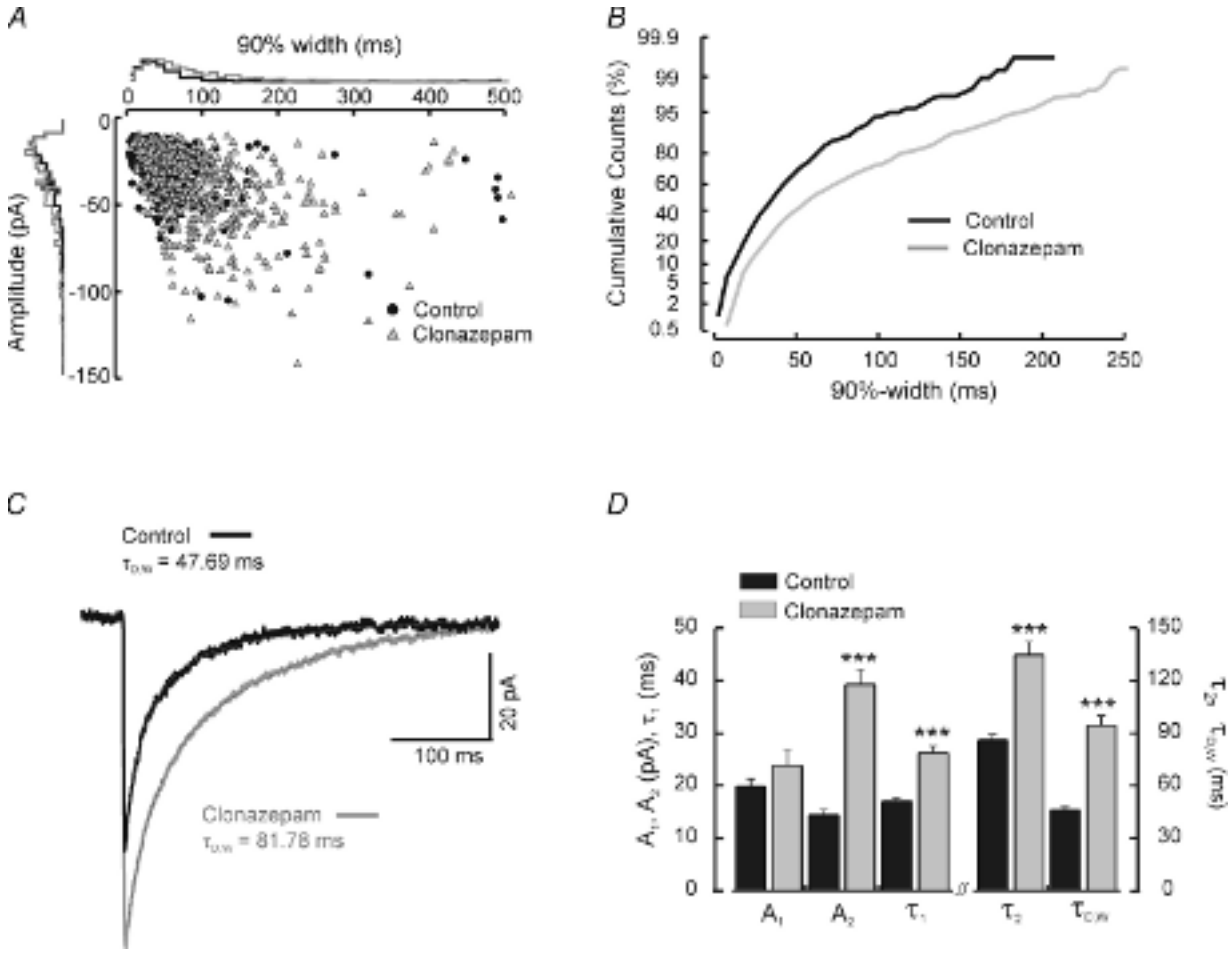

Figure 3. Effects of clonazepam on RTN cell IPSCs
A, scatter plot of 90%-width *versus* amplitude. Each point represents one IPSC obtained from a continuous recording of an RTN cell before (●) and during (▲) bath application of clonazepam. Positioned on the outer side of each axis are normalized histograms of IPSC parameters, either 90%-width (the *x*-axis) or amplitude (the *y*-axis). Clonazepam shifts the overall population to larger and slower events. *B*, cumulative probability histograms of 90%-widths in control and clonazepam for the same cell. *C*, ensemble averaged IPSCs obtained from averaging individual inhibitory events from the control period (black trace, $n = 106$ events) and during bath application of clonazepam (grey trace, $n = 382$ events). The thin dotted line atop each trace represents the double exponential fitted curve. *D*, mean values of amplitude (A_1, A_2) and duration (τ_1, τ_2, $\tau_{D,W}$) from ensemble averaged IPSC traces fitted with two exponentials for control cells (black, $n = 28$) and those either preincubated or exposed to bath application of 100 nM clonazepam (grey, $n = 17$). Level of significance indicated by $***P < 0.0001$. Note that only the amplitude values of the fast decay component (A_1) was unaffected by clonazepam.

RT-PCR are illustrated in Fig. 6. These two cells displayed strikingly different proportions of fast and large events, as can be seen in scattergrams of IPSC decay (90%-width) *versus* amplitude for each neuron (Fig. 6*A* and *B*). The cell in Fig. 6*B* is dominated by IPSCs with fast decay times and large amplitudes, while the cell in Fig. 6*A* has a much higher proportion of small and slow IPSCs. Ensemble averaged IPSCs for each cell were best fitted by the sum of two exponential functions (Fig. 6*C*). The main difference between these two neurons was in the first of two decay components, with a larger amplitude (A_1) and shorter time constant (τ_1) for the ensemble averaged IPSC from the fast cell in Fig. 6*B*.

Single cell amplification of β_1 subunit mRNA was carried out after whole-cell patch-clamp recordings. Reverse transcription and two rounds of PCR amplification were always carried out in the presence of negative (water, pipette solution, lanes 1 and 2, Fig. 6*D*) and positive controls (40 pg of total RNA, lane 8 Fig. 6*D*). All cells were processed on the same day of recording, and therefore if negative and positive controls failed, then all cells were eliminated for that day of experiments. Figure 6*D* shows an example of an ethidium bromide stained polyacrylamide gel with 10 μl of PCR product obtained from cells (lanes 3 through 7) recorded on the same day as the two examples in Fig. 6*A* (lane 3) and 6B (lane 7). Lanes 4, 5 and 6 were from three other RTN neurons. All β_1 positive cells were distinguished by a solitary, 162 bp cDNA product, as predicted by the inner primers of the nested pair. The remainder of the reaction

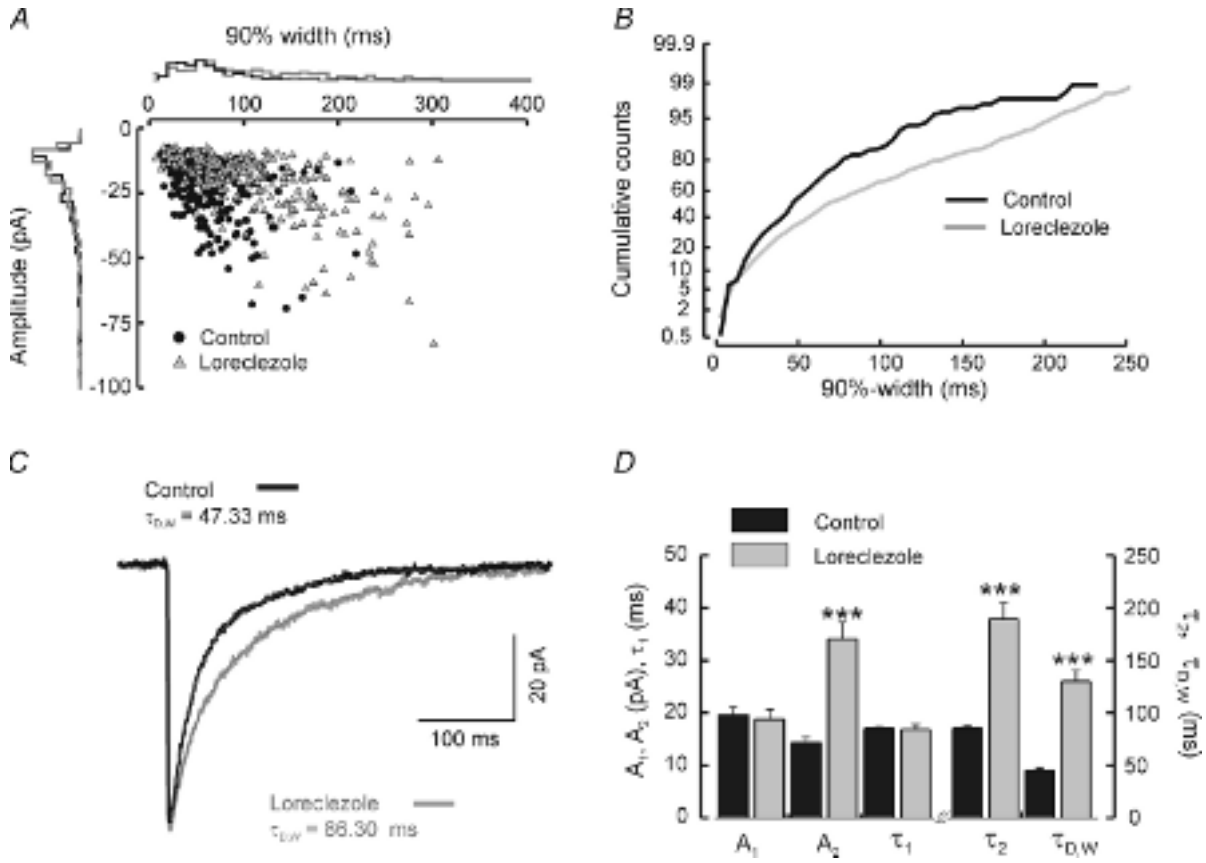

Figure 4. Effects of loreclezole on IPSCs recorded from RTN neurons
A, scatter plot of 90%-width *versus* amplitude in control and after bath application of loreclezole in a single RTN cell. Each point represents an individual IPSC before (●) or during (▲) bath application of loreclezole. Positioned on the outer side of each axis are normalized histograms of either 90%-width (the *x*-axis) or amplitude (the *y*-axis). Loreclezole increased the duration but had little effect on the amplitude of IPSCs. *B*, cumulative probability histograms of 90%-widths for the same cell, taken from periods in the recording before (black graph) and during (grey graph) bath application of 10 μM loreclezole. *C*, ensemble averaged IPSCs from individual inhibitory events averaged together in each trace from the control period (black trace, $n = 144$ events) and during bath application of loreclezole (grey trace, $n = 142$ events). The thin dotted line atop each trace represents the double exponential fitted curve. *D*, mean values of amplitude (A_1, A_2) and duration (τ_1, τ_2, $\tau_{D,W}$) from ensemble averaged IPSC traces fitted with two exponentials for control cells (black, $n = 50$) and cells treated with either bath application or preincubation of loreclezole (grey, $n = 18$). Level of significance indicated by $^{***}P < 0.0001$. Note: the value of neither A_1 nor τ_1 was affected by loreclezole.

product was sequenced and identified as rodent β_1 subunit cDNA by a BLAST (basic local alignment search tool) search in the National Center for Biotechnology Information database.

β_1 positive neurons were distinguished from β_1 negative neurons by faster decay time constants, especially in the fast component of double exponential fitted IPSCs. (Fig. 7). Neurons positive for β_1 mRNA had faster first component time constants (Fig. 7*B*, τ_1: 14.8 ± 0.7 ms, $n = 7$) compared to β_1 negative cells (τ_1: 17.6 ± 0.8 ms, $n = 15$, $P < 0.05$), while amplitudes for the early decay component (A_1) were twice as large in β_1 positive (A_1: 19.9 ± 1.6 pA, $n = 7$) than in negative cells (A_1: 9.8 ± 1.0 pA, $n = 15$, $P < 0.0001$). In β_1 positive cells the mean amplitude of first decay component (A_1) was greater than second component (A_2) by almost twofold (A_1: 19.9 ± 1.6 pA *versus* A_2: 10.4 ± 3.7 pA, $n = 7$, $P < 0.05$), while in β_1 negative cells the two components were of approximately equal weight (A_1: 9.8 ± 1.0 pA *versus* A_2: 9.4 ± 1.1 pA, $n = 17$, $P = 0.8$). Parameters describing the slow decay component were not different between β_1 positive and negative cells (Fig. 7*A*). Overall, the faster and larger fast decay component resulted in a mean weighted time constant ($\tau_{D,W}$) significantly smaller in β_1 positive cells ($\tau_{D,W}$: 35.3 ± 3.2, $n = 7$) than in negative cells ($\tau_{D,W}$: 48.4 ± 2.6 ms, $n = 15$, $P < 0.01$). The limited reduction in the slow component of decay indicates that the significant reductions in $\tau_{D,W}$ were driven by the fast component.

Scatterplots of fast *versus* slow decay components (Fig. 7*B*) show two groups of cells separated by both fast decay times and expression for the β_1 subunit. We then compared these populations to those predicted from the cluster analysis shown in Fig. 1. We found that *all* β_1 positive cells belonged to the fast cluster (cluster 1), but that β_1 negative cells were distributed into both clusters. This latter result suggests the presence of false negatives in the RT-PCR results. If this is the case, then the population data shown in Fig. 7*A* may underestimate the kinetic differences between β_1 containing and β_1 deficient neurons.

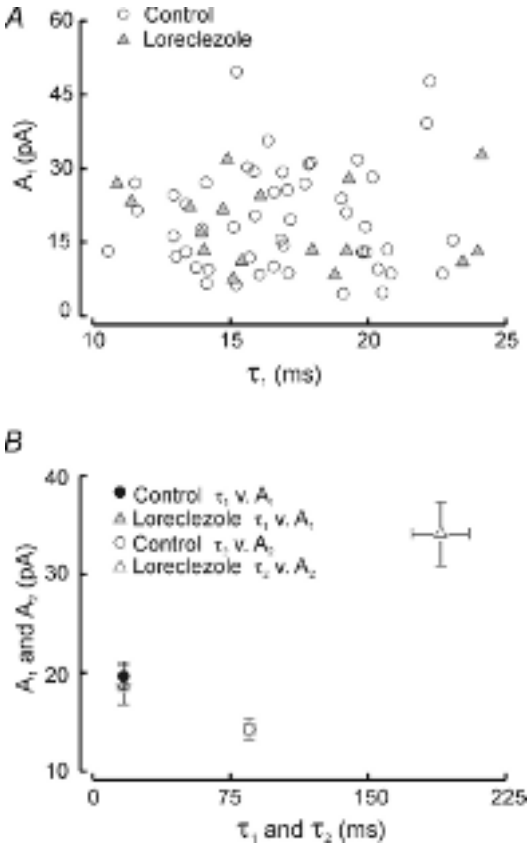

Figure 5. Comparison of the effects of loreclezole on fast and slow IPSC decay
A, scatter plots of fast decay parameters amplitude (A_1) and decay time constant (τ_1) for ensemble averaged IPSCs in control (○) and loreclezole (▲). *B*, mean values of IPSC decay properties (amplitudes *versus* time constants), obtained from double exponential fitted curves. Control τ_1 *versus* A_1 (●), control τ_2 *versus* A_2 (○), loreclezole τ_1 *versus* A_1 (▲) and loreclezole τ_2 *versus* A_2 (△). Error bars represent the standard error of the mean.

Discussion

In the present study, we used a combination of $GABA_A$ receptor subunit-selective pharmacology and single-cell RT-PCR in order to classify RTN neurons with differences in IPSC decay kinetics. We report three principle findings. First, under control conditions, IPSCs recorded from neurons in the RTN have heterogeneous decay properties, with individual neurons exhibiting variable mixtures of rapidly and slowly decaying IPSCs. Cells dominated by faster IPSCs also exhibited large amplitude and/or biphasic events during the recording. Second, we found that two GABA modulating anticonvulsant drugs had differential effects on the degree of IPSC heterogeneity in RTN neurons. The first drug, clonazepam, increased the decay kinetics and overall amplitude, and cumulative probability plots of IPSC durations indicated that all events were prolonged. By contrast, during loreclezole exposure, IPSCs were prolonged but the effect was specific to the second exponential decay component, leaving the first unaffected. Thus brief events with little contribution from the slow component were insensitive (Fig. 4*B*). Third, by using single-cell RT-PCR we found that RTN neurons with large and rapidly decaying IPSCs were much more likely to express β_1 subunit mRNA than those cells with mainly slowly decaying IPSCs.

Heterogeneity of IPSC properties is determined by β_1 subunit expression

In the present study heterogeneous IPSC decay kinetics observed in RTN neurons were defined by differences in both decay rate and amplitude. We conclude that the molecular basis of this heterogeneity was the β_1 subunit.

Given the limited expression of various $GABA_A$ receptor subunits in the RTN, this conclusion is relatively straightforward. Of the more than 19 existing subunits, only four are expressed at significant levels in the RTN: α_3, β_1, β_3 and γ_2 subunits (Wisden *et al.* 1992; Fritschy & Möhler, 1995; Huntsman *et al.* 1996; Pirker *et al.* 2000). This differs from the most common receptor subtype of $\alpha_1\alpha_1\beta_2\beta_2\gamma_2$ (MacDonald & Olsen, 1994; McKernan & Whiting, 1996; Tretter *et al.* 1997). There are variations to this combination of subunits reported in the literature; however, based upon examination of multiple studies using different localization methods (Wisden *et al.* 1992; Fritschy & Möhler, 1995; Huntsman *et al.* 1996; Pirker *et al.* 2000), these four subunits are the most prevalent. Assuming a stoichiometry of $2\alpha2\beta1\gamma$ in any given hetero-multimeric synaptic receptor (Tretter *et al.* 1997; Klausberger *et al.* 2001), then $GABA_A$ receptors in the RTN are likely to consist of three closely related possibilities: $\alpha_3\alpha_3\beta_1\beta_1\gamma_2$, $\alpha_3\alpha_3\beta_1\beta_3\gamma_2$ or $\alpha_3\alpha_3\beta_3\beta_3\gamma_2$.

To narrow down this pool we selected two antiepileptic drugs that target different sites on the $GABA_A$ receptor. The benzodiazepine clonazepam was chosen because α subunits determine benzodiazepine responsiveness (Pritchett *et al.* 1989). In the RTN, the likely target is the α_3 subunit. This is based on a combination of studies that examine subunit localization. While it is conceivable

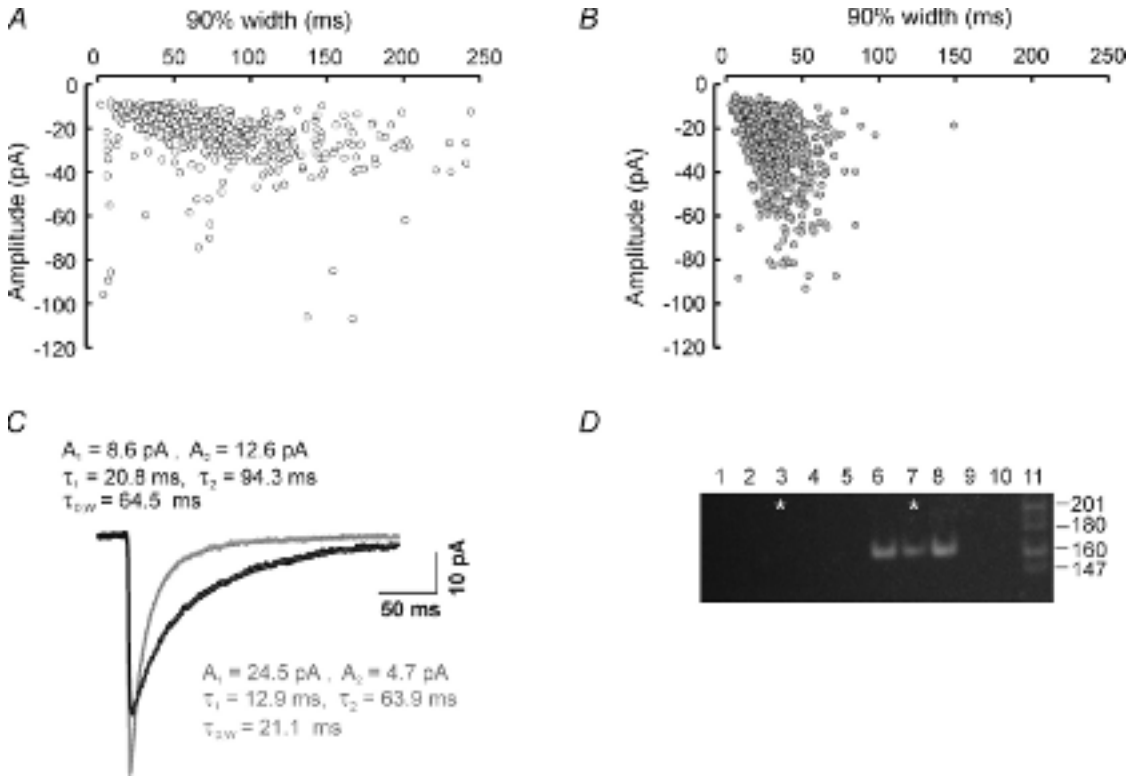

Figure 6. Cells with fast initial decay kinetics express β_1 subunit mRNA
A and *B*, scatter plots of IPSC 90%-width versus peak current amplitude for two RTN cells recorded on the same day. Each point in *A* and *B* represents an individual IPSC. *A* is a recording from a cell dominated with slow and small IPSCs (○) and *B*, represents a recording dominated by brief and large IPSCs (●). *C*, ensemble averaged IPSCs averaged from isolated spontaneous inhibitory events (selected on the basis of having arisen from an event-free baseline and showing complete decay to the same baseline) for the two cells represented in *A* (black, $n = 258$) and *B* (grey, $n = 217$). Each trace was best fitted to two exponentials (dotted line superimposed on each trace). Note: the cell dominated with fast IPSCs yielded a ensemble averaged IPSC with a larger A_1 value than A_2 whereas the opposite is true for the slower cell. *D*, ethidium bromide stained 8% polyacrylamide gel showing single-cell RT-PCR analysis from five RTN cells examined in one day of recording, two of the cells are represented in *A* (lane 3) and *B* (lane 7). Cells positive for the β_1 subunit cDNA showed a solitary band at 162 bp after two rounds of amplification using nested primers (lanes 6 and 7, see methods). Lanes 1 and 2 are water and media controls that underwent reverse transcription along with individual cells in lanes 3 through 7; lane 8 is a positive control using 40 pg of total RNA; lanes 9 and 10 are water controls used in the master mix for each round of PCR amplification. The molecular weight marker in lane 11 is the *Msp*I digest of pBR322. The size of each fragment is noted on the right. The parameters for β_1 negative cells in lane 4: $A_1 = 9.80$, $\tau_1 = 13.75$, $A_2 = 14.17$, $\tau_2 = 64.61$, $\tau_{DW} = 43.82$l; and lane 5: $A_1 = 12.94$, $\tau_1 = 12.94$, $A_2 = 5.69$, $\tau_2 = 77.21$, $\tau_{DW} = 29.63$. The β_1 positive cell in lane 6: $A_1 = 18.05$, $\tau_1 = 15.11$, $A_2 = 4.15$, $\tau_2 = 74.44$, $\tau_{DW} = 26.20$.

that another α subunit (possibly α_1) may contribute to the fast component, this can be eliminated if one takes into account a number of factors. First, two studies (one immunocytochemical and one of *in situ* mRNA localization) report that α_3 is the only α subunit identified in the RTN (excluding the cerebellar α_6 subunit; Fritschy & Möhler, 1995; Huntsman *et al.* 1996). Second, two other studies indicate that α_3 is the primary α subunit with lower levels of α_1 mRNA and protein (Pirker *et al.* 2000).

Additional data obtained with $GABA_A$ receptor mutant mice provide further support for a primary, if not exclusive, role for α_3 subunits in RTN synaptic $GABA_A$ receptors. Recordings from RTN cells in a mouse strain in which the diazepam binding site on the α_3 subunit gene has been inactivated by a point mutation (α3H126R, Low *et al.* 2000) demonstrated that clonazepam increased the duration of $GABA_A$ receptor-mediated IPSCs in wild-type but not α3H126R RTN cells (Porcello *et al.* 2001). By contrast, the modulatory actions of clonazepam were completely intact in RTN cells of α1H101R mice (Huntsman *et al.* 2000), in which the α_1 subunit was rendered benzodiazepine-insensitive by a single point mutation (Rudolph *et al.* 1999).

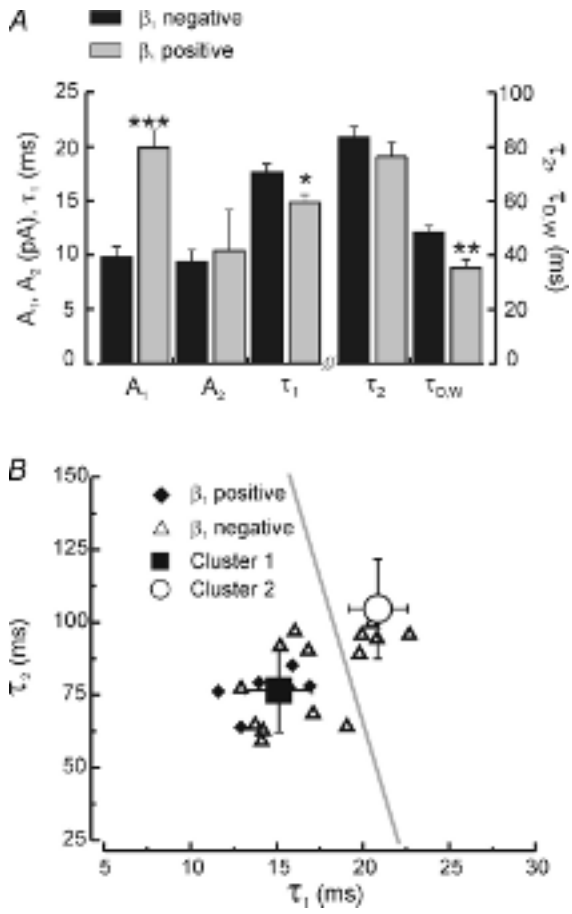

Figure 7. RTN cells positive for the β_1 subunit are distinguishable by their initial decay kinetics
A, mean values of amplitude (A_1, A_2) and duration (τ_1, τ_2, $\tau_{D,W}$) from ensemble averaged IPSC traces fitted with two exponentials for β_1 negative cells (black bars, $n = 17$) and β_1 positive cells (grey bars, $n = 7$). Note the larger A_1 and faster τ_1 and $\tau_{D,W}$-values for β_1 positive cells. *B*, scatter plots of fast and slow decay components from β_1 negative (△) and β_1 positive cells (♦). Mean values (group 1 ■, group 2 ○) from the cluster analysis in Fig. 1 are also plotted (error bars indicate standard deviation), as is the cluster division line (grey), obtained from the discriminant function with a critical *Z*-score of 0.85. Note β_1 negative cells (△) that fall into the group 1–fast cluster, suggest the possibility of 'false negatives'. Level of significance indicated by $^{***}P < 0.0001$, $^{**}P < 0.01$, $^{*}P < 0.05$.

In the present study, application of clonazepam to thalamic slices increased the duration and amplitude of IPSCs; however, the degree of heterogeneity in the overall population of events, as measured by the curvature in the cumulative probability plots, was not greatly altered. This suggests that all IPSCs, both brief and long-lasting events, were modulated by clonazepam, and that the receptors underlying fast and slow decay were similarly sensitive, as might be expected if all such receptors contained two copies of the α_3 subunit.

In contrast to clonazepam, loreclezole sensitivity is determined primarily by the β subunits, with β_2- and β_3-, but not β_1-containing receptors being highly sensitive (Wafford *et al.* 1994; Wingrove *et al.* 1994). Because neurons in this nucleus completely lack β_2 message (Huntsman *et al.* 1996), loreclezole effects should depend completely on the β_3 subunit. The effect of loreclezole in RTN cells was an overall increase in the duration of IPSCs. Analysis of double exponential fits of ensemble averaged IPSCs revealed that this enhancement was achieved mainly through prolongation of the slowly decaying component leaving the fast component completely unaffected (Fig. 5*B*). This is perhaps the strongest evidence in this report for differential involvement of β subunits in fast *versus* slow decay components of RTN IPSCs. Notably, some IPSCs still showed a prominent fast decay component, even after several minutes of loreclezole exposure with bath application or preincubation, thus suggesting that two populations of $GABA_A$ receptors, β_1 containing and β_1 deficient, can coexist at individual synapses in RTN. While α subunits have been shown to regulate the duration of GABA responses (Gingrich *et al.* 1995; Verdoorn, 1994; Lavoie *et al.* 1997; Serafini *et al.* 1998), the role of β subunits in this context has not been fully studied. However, the β subunits have been shown to influence the rate of desensitization (Burgard *et al.* 1996). In that study, recombinant receptors with α_5, β, and γ_2L subunits had different desensitization rates (at hyperpolarized potentials) with the following rank order of desensitization rates: $\beta_2 > \beta_1 > \beta_3$. Both β and α subunits make up the structural domain for the GABA binding site (Amin & Weis, 1993), and thus both may influence binding affinity. It is apparent that changes in GABA affinity

coincide with the β subunit (Hadingham *et al.* 1993; Ebert *et al.* 1994; Ducic *et al.* 1995), with β_3 containing receptors having a much higher GABA affinity than β_1 containing receptors (Burgard *et al.* 1996). This may be important since it has been noted by Jones *et al.* (1998) that the binding of GABA is especially critical at low GABA concentrations and that 'receptors that mediate fast IPSCs may be less efficient at binding GABA and thus have a lower occupancy than those underlying slower IPSCs' (Jones *et al.* 1998). Further support for differential roles of β_1 and β_3 receptor subunits in mediating fast and slow IPSCs, respectively, comes from the finding that residual IPSCs in RTN cells of β_3 knockout mice consist of a uniform population of rapidly decaying events (Huntsman *et al.* 1999), quite different from the heterogeneous distribution of IPSCs observed in wild-type mice. Furthermore, mIPSC durations are shortened in cortical neurons of mice devoid of β_3 subunits (Ramadan *et al.* 2003). Even though these data suggest a direct role for β_1 subunits in the regulation of IPSC duration, other factors that could also influence IPSC duration such as phosphorylation, release sites or receptor occupancy have not been explicitly studied here (Poisbeau *et al.* 1999; Hinkle & Macdonald, 2003).

$GABA_A$ receptor mRNA expression is extremely low in the RTN (Huntsman *et al.* 1996), thus creating a formidable technical challenge when attempting to successfully amplify specific subunit messages. The design of an experiment with single RT-PCR amplification of one product was crucial to the success of the study. In a previous study from this laboratory using multiplex PCR and nested primers (Browne *et al.* 2001), we were unable to detect message for any β subunits in RTN cells, even though both β_1 and β_3 have been previously detected in this nucleus (Wisden *et al.* 1992; Huntsman *et al.* 1996; Pirker *et al.* 2000). Our results are consistent with occasional false negatives (Fig. 7*B*) whose incidence may be higher than that expected from other single cell RT-PCR studies (Brorson *et al.* 1999; van Hooft *et al.* 2000). Even with these putative false negatives included in the β_1-negative pool, the two cell populations exhibited significantly different IPSC decay kinetics (Fig. 7*A*), supporting the robustness of the result.

Functional heterogeneity requires minimal variation of $GABA_A$ receptor subtypes

Why would a brain region that is highly dependent upon $GABA_A$ receptor-mediated postsynaptic inhibition for normal function (Ulrich & Huguenard, 1996; Sanchez-Vives *et al.* 1997; Huntsman *et al.* 1999) limit its functional capabilities by expressing only a few receptor subtypes? Supernumerary subunit expression is common in many brain regions and appears redundant but is likely to be the basis for functional diversity of $GABA_A$ receptor mediated synaptic events observed in various regions (Otis & Mody, 1992; Mody *et al.* 1994; Tia *et al.* 1996; Galarreta & Hestrin, 1997; Hollrigel & Soltesz, 1997; Nusser *et al.* 1997; Zhang *et al.* 1997; Banks *et al.* 1998; Xiang *et al.* 1998; Bai *et al.* 1999; Brickley *et al.* 1999; Perrais & Ropert, 1999; Banks & Pearce, 2000; Huntsman & Huguenard, 2000; Hutcheon *et al.* 2000). However, in contrast to other regions that have large numbers of coexpressed $GABA_A$ receptor subunits (e.g. neocortex, amygdala, hippocampus), the RTN is one region where receptor subunit overlap is minimal and overall expression levels are very low (Huntsman *et al.* 1996). This limited expression should dictate a limited range of synaptic responses, yet our data suggest that significant functional heterogeneity is obtained, even in single RTN neurons. It is likely that a significant contributor to such heterogeneity is the presence or absence of perhaps a single copy of the β_1 subunit.

Basis and function of heterogeneous IPSCs in the RTN

Variability in RTN neuron IPSCs would have important physiological consequences for both intra-thalamic and thalamocortical interactions. Intra-RTN inhibition mainly relies on slowly decaying $GABA_A$ receptor mediated IPSCs. The majority of inhibitory synapses in rodent RTN arise from sparse axon collaterals of other RTN neurons (Scheibel & Scheibel, 1966; Deschênes *et al.* 1985; Yen *et al.* 1985; Cox *et al.* 1996; Pinault *et al.* 1997; Steriade *et al.* 1997). There is also evidence for extrinsic GABAergic input to the RTN – mainly arising from the globus pallidus, basal forebrain, and the substantia nigra pars reticulata (Asanuma & Porter, 1990; Paré *et al.* 1990; Hazrati & Parent, 1991; Asanuma, 1994). However, pathway specific inhibition is not likely to contribute to heterogeneous IPSC decay rates. For example, a higher proportion of rapidly decaying IPSCs might arise from extrinsic *versus* intrinsic inhibitory connections). Extrinsic GABAergic projections typically make up a minor proportion of synaptic contacts in comparison to the connections arising within the RTN and are often segregated and located in different sectors of the nucleus (Paré *et al.* 1990; Steriade *et al.* 1997). We found that neurons with heterogeneous IPSCs occurred throughout the RTN and were not located in a defined location.

The difference in IPSC duration (measured by $\tau_{D,W}$ at room temperature) between β_1 positive and β_1 negative neurons is roughly 13 ms (this is all cells examined with single cell PCR, including the presumed false negatives). Why might a 13-ms difference make a difference? In the hippocampus, the precise timing of fast $GABA_A$ receptor mediated IPSCs is required for the synchronization of neuronal networks (Buzáki *et al.* 1983; Soltesz & Deschênes, 1993; Whittington *et al.* 1995). Dual modelling

and physiological results indicate that the generation of oscillatory networks depends on a narrow range of (6–12 ms) IPSC decay (Whittington *et al.* 1995). The synapses between inhibitory neurons in particular, appear to require a fast conductance change (mediated by fast decay and large amplitude IPSCs) for the generation of synchronized network activity in the gamma frequency range (Bartos *et al.* 2001). A large initial amplitude and fast decay is also a feature of β_1 positive neurons in the RTN and may play a role in the observed voltage-dependent 40-Hz oscillations in this nucleus (Pinault & Deschênes, 1992). Target specific expression of $GABA_A$ receptor subunits is an emerging characteristic feature in inhibitory networks (Nyiri *et al.* 2001; Klausberger *et al.* 2002; Bacci *et al.* 2003).

Inhibitory connections within the RTN are likely to be important in controlling the inhibitory output of this nucleus *in vitro* (von Krosigk *et al.* 1993; Huguenard & Prince, 1994; Sanchez-Vives *et al.* 1997). This is a controversial issue since RTN connections have been proposed to both dampen and facilitate oscillations (Ahlsén & Lindström, 1982; Steriade *et al.* 1987; Huguenard & Prince, 1994; Sanchez-Vives *et al.* 1997; Huntsman *et al.* 1999). While these synapses are seemingly few in number, if compromised they can transform thalamic activity from partially synchronous spindle-type activity to hyper-synchronous epileptiform responses (von Krosigk *et al.* 1993; Huguenard & Prince, 1994; Bal *et al.* 1995; Huntsman *et al.* 1999; Sohal *et al.* 2000). As mentioned above, reduced inhibitory function was observed in RTN neurons from β_3-subunit knockout mice (Huntsman *et al.* 1999). This reduction was manifest as very small amplitude IPSCs, with reduced frequency and fast IPSC decay kinetics. In a related modelling study, we found that slow decay of IPSCs in RTN neurons was critical in restricting intrathalamic activity to particular spatiotemporal patterns, thus preventing epileptiform activity (Sohal *et al.* 2000). RTN neurons are also active during wakefulness, for example in the processing of ascending sensory neurotransmission. It has been shown that RTN neurons in specific sectors respond to activation of adjacent sensory relay nuclei (Jones, 1975; Yen *et al.* 1985; Hartings *et al.* 2000). Whether or not intra-RTN inhibition plays a role in the restriction of these sectors during peripheral stimulation (e.g. whisker movement) remains to be shown. Nevertheless, we speculate that the presence of β_1 subunits in $GABA_A$ receptors allows for a wider dynamic range of inhibitory function that would be relevant to sensory processing or in states of focused arousal (Pinault & Deschênes, 1992; Hartings *et al.* 2000). Taken together with the likely existence of electrical connections between RTN neurons (Landisman *et al.* 2002), the seemingly 'limited' RTN inhibitory synapses may have an even wider range of inhibitory function then first proposed.

References

Ahlsén G & Lindström S (1982). Mutual inhibition between perigeniculate neurons. *Brain Res* **236**, 482–486.

Amin J & Weiss DS (1993). $GABA_A$ receptor needs two homologous domains of the β-subunit for activation of GABA but not for pentobarbital. *Nature* **366**, 5665–5569.

Asanuma C (1994). GABAergic and pallidal terminals in the thalamic reticular nucleus of squirrel monkeys. *Exp Brain Res* **101**, 439–451.

Asanuma C & Porter LL (1990). Light and electron microscopic evidence for a GABAergic projection from the caudal basal forebrain to the thalamic reticular nucleus in rats. *J Comp Neurol* **302**, 159–172.

Bacci A, Rudolph U, Huguenard JR & Prince DA (2003). Major differences in inhibitory synaptic transmission onto two neocortical interneuron subclasses. *J Neurosc* **23**, 9664–9674.

Bai D, Pennefather PS, MacDonald JF & Orser BA (1999). The general anesthetic propofol slows deactivation and desensitization of $GABA_A$ receptors. *J Neurosci* **19**, 10635–10646.

Bal T, von Krosig M & McCormick DA (1995). Role of ferret perigeniculate nucleus in the generation of synchronized oscillations *in vitro*. *J Physiol* **483**, 665–685.

Banks MI, Li T-B & Pearce RA (1998). The synaptic basis of $GABA_{A,slow}$. *J Neurosci* **18**, 1305–1317.

Banks MI & Pearce RA (2000). Kinetic differences between synaptic and extrasynaptic $GABA_A$ receptors in CA1 pyramidal cells. *J Neurosci* **20**, 937–948.

Bartos M, Vida I, Frotscher M, Geiger JRP & Jonas P (2001). Rapid signaling at inhibitory synapses in a dentate gyrus interneuron network. *J Neurosci* **21**, 2687–2698.

Berger T, Schwarz C, Kraushaar U & Monyer H (1998). Dentate gyrus basket cell $GABA_A$ receptors are blocked by Zn^{2+} via changes of their desensitization kinetics: an in situ patch-clamp and single-cell PCR study. *J Neurosci* **18**, 2437–2448.

Brickley SG, Cull-Candy SG & Farrant M (1999). Single-channel properties of synaptic and extrasynaptic $GABA_A$ receptors suggest differential targeting of receptor subtypes. *J Neurosci* **19**, 2960–2973.

Brorson JR, Zhang Z & Vandenberghe W (1999). Ca^{2+} permeation of AMPA receptors in cerebellar neurons expressing Glu receptor 2. *J Neurosci* **19**, 9149–9159.

Browne SH, Kang J, Akk G, Chiang LW, Schulman H, Huguenard JR & Prince DA (2001). Kinetic and pharmacological properties of $GABA_A$ receptors in single thalamic neurons and $GABA_A$ subunit expression. *J Neurophysiol* **86**, 2312–2322.

Burgard EC, Tietz EI, Neelands TR & Macdonald RL (1996). Properties of recombinant γ-aminobutyric $acid_A$ receptor isoforms containing the α5 subunit subtype. *Mol Pharmacol* **50**, 119–127.

Buzáki G, Leung LW & Vanderwolf CH (1983). Cellular basis of hippocampal EEG in the behaving rat. *Brain Res* **287**, 139–171.

Cox CL, Huguenard JR & Prince DA (1996). Heterogeneous axonal arborizations of rat thalamic reticular neurons in the ventrobasal nucleus. *J Comp Neurol* **366**, 416–430.

Deschênes M, Madariaga-Domich A & Steriade M (1985). Dendrodendritic synapses in the cat reticular thalami nucleus: a structural basis for thalamic spindle synchronization. *Brain Res* **334**, 165–168.

Draguhn A & Heinemann U (1996). Different mechanisms regulate IPSC kinetics in early postnatal and juvenile hippocampal granule cells. *J Neurophysiol* **76**, 3983–3993.

Ducic I, Caruncho HJ, Zhu WJ, Vicini S & Costa E (1995). γ-Aminobutyric acid gating of Cl^- channels in recombinant $GABA_A$ receptors. *J Pharmacol Exp Ther* **272**, 438–445.

Ebert B, Wafford KA, Whiting PJ, Krogsgaard-Larsen P & Kemp JA (1994). Molecular pharmacology of γ-aminobutyric acid type A receptor agonists and partial agonists in oocytes injected with different α, β, and γ receptor subunit combinations. *Mol Pharmacol* **46**, 957–963.

Fritschy J-M & Möhler H (1995). $GABA_A$-receptor heterogeneity in the adult rat brain: Differential regional and cellular distribution of seven major subunits. *J Comp Neurol* **359**, 154–194.

Galarreta M & Hestrin S (1997). Properties of $GABA_A$ receptors underlying inhibitory synaptic currents in neocortical pyramidal cells. *J Neurosci* **17**, 7220–7227.

Garden DL, Kemp N & Bashir ZI (2002). Differences in GABAergic transmission between two inputs into the perirhinal cortex. *Eur J Neurosci* **16**, 437–444.

Ghavanini AA, Mathers DA & Puil E (2005). Glycinergic inhibition in thalamus revealed by synaptic receptor blockade. *J Neuropharm* **49**, 338–349.

Gingrich KJ, Roberts WA & Kass RS (1995). Dependence of the $GABA_A$ receptor gating kinetics on the α-subunit isoform: implications for structure–function relations and synaptic transmission. *J Physiol* **489**, 529–543.

Hadingham KL, Wingrove PB, Wafford KA, Bain C, Kemp JA *et al.* (1993). Role of the β subunit in determining the pharmacology of human γ-aminobutyric acid type A receptors. *Mol Pharmacol* **44**, 1121–1218.

Hájos N, Nusser Z, Rancz EA, Freund TF & Mody I (2000). Cell type- and synapse-specific variability in synaptic $GABA_A$ receptor occupancy. *Eur J Neurosci* **12**, 810–818.

Hartings JA, Temereanca S & Simons DJ (2000). High responsiveness and direction sensitivity of neurons in the rat thalamic reticular nucleus to vibrissa deflections. *J Neurophysiol* **83**, 2791–2801.

Hazrati L-N & Parent A (1991). Projection from the external pallidum to the reticular thalamic nucleus in the squirrel monkey. *Brain Res* **550**, 142–146.

Hefti BJ & Smith PH (2000). Anatomy, physiology, and synaptic responses of rat layer V auditory cortical cells and effects of intracellular $GABA_A$ blockade. *J Neurophysiol* **83**, 2626–2638.

Hinkle DJ & Macdonald RL (2003). β subunit phosphorylation selectively increases fast desensitization and prolongs deactivation of $\alpha1\beta1\gamma2$L and $\alpha1\beta3\gamma2$L $GABA_A$ receptor currents. *J Neurosci* **23**, 11698–11710.

Hollrigel GS & Soltesz I (1997). Slow kinetics of miniature IPSCs during early postnatal development in granule cells of the dentate gyrus. *J Neurosci* **17**, 5119–5128.

Hollrigel GS, Toth K & Soltesz I (1996). Neuroprotection by propofol in acute mechanical injury: role of GABAergic inhibition. *J Neurophysiol* **76**, 2412–2422.

Houser CR, Vaughn JE, Barber RP & Roberts E (1980). GABA neurons are the major cell type of the nucleus reticularis thalami. *Brain Res* **200**, 341–354.

Huguenard JR & Prince DA (1994). Clonazepam suppresses $GABA_B$-mediated inhibition in thalamic relay neurons through effects in nucleus reticularis. *J Neurophysiol* **71**, 2576–2581.

Huntsman MM & Huguenard JR (2000). Nucleus-specific differences in $GABA_A$ receptor-mediated inhibition are enhanced during thalamic development. *J Neurophysiol* **83**, 350–358.

Huntsman MM & Huguenard JR (2001). Subunit selective basis for differential pharmacology of fast and slow inhibition in the thalamic reticular nucleus. *Soc Neurosci Abs* **27**, 491.4.

Huntsman MM, Leggio ML & Jones EG (1996). Nucleus-specific expression of ten $GABA_A$ receptor subunit mRNAs in monkey thalamus. *J Neurosci* **16**, 3571–3589.

Huntsman MM, Porcello DM, Homanics GE, DeLorey TM & Huguenard JR (1999). Reciprocal inhibitory connections and network synchrony in the mammalian thalamus. *Science* **283**, 541–543.

Huntsman MM, Porcello DM, Rudolph U & Huguenard JR (2000). $GABA_A$ receptor mutant mice reveal subtype-selective benzodiazepine modulation of inhibitory synaptic responses in thalamic neurons. *Soc Neurosci Abs* **26**, 55.23.

Hutcheon B, Morley P & Poulter MO (2000). Developmental change in $GABA_A$ receptor desensitization kinetics and its role in synapse function in rat cortical neurons. *J Physiol* **522**, 3–17.

Inoue M, Duysens J, Vossen JM & Coenen AM (1993). Thalamic multiple-unit activity underlying spike-wave discharges in anesthetized rats. *Brain Res* **612**, 35–40.

Jones EG (1975). Some aspects of the organization of the thalamic reticular complex. *J Comp Neurol* **162**, 285–308.

Jones EG (1985). *The Thalamus*. Plenum, New York.

Jones MV, Sahara Y, Dzubay JA & Westbrook GL (1998). Defining affinity with the $GABA_A$ receptor. *J Neurosci* **18**, 8590–8604.

Jones MV & Westbrook GL (1995). Desensitized states prolong $GABA_A$ channel responses to brief agonist pulses. *Neuron* **15**, 181–191.

Jones MV & Westbrook GL (1997). Shaping of IPSCs by endogenous calcineurin activity. *J Neurosci* **17**, 7626–7633.

Klausberger T, Roberts JDB & Somogyi P (2002). Cell type and input-specific differences in the number and subtypes of synaptic $GABA_A$ receptors in the hippocampus. *J Neurosci* **22**, 2513–2521.

Klausberger T, Sarto I, Ehya N, Fuchs K, Furtmüller R, Mayer B *et al.* (2001). Alternate use of distinct intersubunit contacts controls $GABA_A$ receptor assembly and stoichiometry. *J Neurosci* **21**, 9124–9133.

Kobayashi M & Buckmaster PS (2003). Reduced inhibition of dentate granule cells in a model of temporal lobe epilepsy. *J Neurosci* **23**, 2440–2452.

Landisman CE, Long MA, Beierlein M, Deans MR, Paul DL & Connors BW (2002). Electrical synapses in the thalamic reticular nucleus. *J Neurosci* **22**, 1002–1009.

Lavoie AM, Tingey JJ, Harrison NL, Pritchett DB & Twyman RE (1997). Activation and deactivation rates of recombinant $GABA_A$ receptor channels are dependent on α-subunit isoforms. *Biophys J* **73**, 2518–2526.

Low K, Crestani F, Keist R, Benke D, Brunig I, Benson JA *et al.* (2000). Molecular and neuronal substrate for the selective attenuation of anxiety. *Science* **290**, 131–134.

MacDonald RL & Olsen RW (1994). $GABA_A$ receptor channels. *Ann Rev Neurosci* **17**, 569–602.

Maconochie DJ, Zempel JM & Steinbach JH (1994). How quickly can $GABA_A$ receptors open? *Neuron* **12**, 61–71.

Massengill JL, Smith MA, Son DI & O'Dowd DK (1997). Differential expression of K4-AP currents and Kv3.1 potassium channel transcripts in cortical neurons that develop distinct firing phenotypes. *J Neurosci* **17**, 3136–3147.

McKernan RM & Whiting PJ (1996). Which $GABA_A$ receptor subtypes really occur in the brain? *Trends Neurosci* **19**, 139–143.

Mody I, De Konninck Y, Otis TS & Soltesz I (1994). Bridging the cleft at GABA synapses in the brain. *Trends Neurosci* **17**, 517–525.

Monyer H & Jonas P (1995). Polymerase chain reaction analysis of ion channel expression in single neurons of brain slices. In *Single-Channel Recording*, ed. Sakmann B & Neher E, pp. 357–373. Plenum Press, New York.

Nusser Z, Cull-Candy S & Farrant M (1997). Differences in synaptic $GABA_A$ receptor number underlie variation in GABA mini amplitude. *Neuron* **19**, 697–709.

Nyiri G, Freund TF & Somogyi P (2001). Input-dependent synaptic targeting of γ2-containing $GABA_A$ receptors in synapses of hippocampal pyramidal cells of the rat. *Eur J Neurosci* **13**, 428–442.

Okada M, Onodera K, Van Rebterghem C, Sieghart W & Takahashi T (2000). Functional correlation of $GABA_A$ receptor α subunits expression with the properties of IPSCs in the developing thalamus. *J Neurosci* **20**, 2202–2208.

Otis TS & Mody I (1992). Modulation of decay kinetics and frequency of $GABA_A$ receptor-mediated spontaneous inhibitory postsynaptic currents in hippocampal neurons. *Neuroscience* **49**, 13–32.

Paré D, Hazrati L-N, Parent A & Steriade M (1990). Substantia nigra pars reticulata projects to the reticular thalamic nucleus of the cat: a morphological and electrophysiological study. *Brain Res* **535**, 139–146.

Perrais D & Ropert N (1999). Effect of zolpidem on miniature IPSCs and occupancy of postsynaptic $GABA_A$ receptors in central synapses. *J Neurosci* **19**, 578–588.

Pinault D & Deschênes M (1992). Voltage-dependent 40-Hz oscillations in rat reticular thalamic neurons in vivo. *Neuroscience* **51**, 245–258.

Pinault D, Smith Y & Deschênes M (1997). Dedrodendritic and axoaxonic synapses in the thalamic reticular nucleus of the adult rat. *J Neurosci* **17**, 3215–3233.

Pirker S, Schwarzer C, Wieselthaler A, Sieghart W & Sperk G (2000). $GABA_A$ receptors: immunocytochemical distribution of 13 subunits in the adult rat brain. *Neuroscience* **101**, 815–850.

Poisbeau P, Cheney MC, Browning MD & Mody I (1999). Modulation of synaptic $GABA_A$ receptor function by PKA and PKC in adult hippocampal neurons. *J Neurosci* **19**, 674–683.

Porcello DM, Huntsman MM, Keist R, Rudolph U & Huguenard JR (2001). $GABA_A$ receptor mutant mice reveal subtype selective benzodiazepine modulation of intra-inhibitory connections in reticular thalamus. *Soc Neurosci Abs* **27**, 491.3.

Pritchett DB, Lüddens H & Seeburg PH (1989). Type I and Type II $GABA_A$-benzodiazepine receptors produced in transfected cells. *Science* **245**, 1389–1392.

Puia G, Vicini S, Seeburg PH & Costa E (1991). Influence of recombinant gamma-aminobutyric acid-A receptor subunit composition on the action of allosteric modulators of gamma-aminobutyric acid-gated Cl^- currents. *Mol Pharmacol* **39**, 691–696.

Ramadan E, Fu Z, Losi G, Homanics GE, Neale JH & Vicini S (2003). $GABA_A$ receptor β3 subunit deletion decreases α2/3 subunits and IPSC duration. *J Neurophysiol* **89**, 128–134.

Rudolph U, Crestani F, Benke D, Brünig I, Benson JA, Fritschy JM *et al.* (1999). Benzodiazepine actions mediated by specific gamma-aminobutyric acid-A receptor subtypes. *Nature* **401**, 796–800.

Sanchez-Vives MV, Bal T & McCormick DA (1997). Inhibitory interactions between perigeniculate GABAergic neurons. *J Neurosci* **17**, 8894–8908.

Sanchez-Vives MV & McCormick DA (1997). Functional properties of perigeniculate inhibition of dorsal lateral geniculate nucleus thalamocortical neurons in vitro. *J Neurosci* **17**, 8880–8893.

Scheibel ME & Scheibel AB (1966). The organization of the nucleus reticularis thalami: a Golgi study. *Brain Res* **1**, 43–62.

Serafini R, Maric D, Maric I, Ma W, Fritschy J-M, Zhang L & Barker JL (1998). Dominant $GABA_A$ receptor/Cl^- channel kinetics correlate with the relative expressions of α_2, α_3, α_5 and β_3 subunits in embryonic rat neurons. *Eur J Neurosci* **10**, 334–349.

Sohal VS, Huntsman MM & Huguenard JR (2000). Reciprocal inhibitory connections regulate the spatiotemporal properties of intrathalamic oscillations. *J Neurosci* **20**, 1735–1745.

Soltesz I & Deschênes M (1993). Low- and high-frequency membrane potential oscillations during theta activity in CA1 and CA3 pyramidal neurons in the rat hippocampus under ketamine-xylazine anesthesia. *J Neurophysiol* **70**, 97–116.

Steriade M, Domich L, Oakson G & Deschênes M (1987). The deafferented reticular thalamic nucleus generates spindle rhythmicity. *J Neurophysiol* **57**, 260–273.

Steriade M, Jones EG & McCormick DA (1997). *Thalamus*, vol. 1, *Organization and Function*, pp. 252–255. Elsevier Science Ltd, Oxford, UK.

Sucher NJ, Deitcher DL, Baro DJ, Harris Warrick RM & Guenther E (2000). Genes and channels: Patch/voltage-clamp analysis and single-cell RT-PCR. *Cell Tissue Res* **302**, 295–307.

Tia S, Wang JF, Kotchabhakdi N & Vincini S (1996). Developmental changes of inhibitory synaptic currents in cerebellar granule neurons: role of $GABA_A$ receptor α6 subunit. *J Neurosci* **16**, 3630–3640.

Tretter V, Ehya N, Fuchs K & Sieghart W (1997). Stoichiometry and assembly of a recombinant $GABA_A$ receptor subtype. *J Neurosci* **17**, 2728–2737.

Ulrich D & Huguenard JR (1996). $GABA_B$-receptor-mediated responses in GABAergic projection neurons of rat nucleus reticularis thalami *in vitro*. *J Physiol* **493**, 845–854.

Ulrich D & Huguenard JR (1997). $GABA_A$-receptor-mediated rebound burst firing and burst shunting in thalamus. *J Neurophysiol* **78**, 1748–1751.

van Hooft JA, Giuffrida R, Blatow M & Monyer H (2000). Differential expression of group I metabotropic glutamate receptors in functionally distinct hippocampal neurons. *J Neurosci* **20**, 3544–3551.

Verdoorn TA (1994). Formation of heteromeric γ-aminobutyric acid type-A receptors containing two different α subunits. *Mol Pharmacol* **45**, 475–480.

Vicini S, Ferguson C, Prybylowski K, Kralic J, Morrow AL & Homanics GE (2001). $GABA_A$ receptor $\alpha 1$ subunit deletion prevents developmental changes of inhibitory synaptic currents in cerebellar neurons. *J Neurosci* **21**, 3009–3016.

von Krosigk M, Bal T & McCormick DA (1993). Cellular mechanisms of a synchronized oscillation in the thalamus. *Science* **261**, 361–364.

Wafford KA, Bain CJ, Quirk K, McKernan RM, Wingrove PB, Whiting PJ & Kemp JA (1994). A novel allosteric modulatory site on the $GABA_A$ receptor β subunit. *Neuron* **12**, 775–782.

Whittington MA, Traub RD & Jefferys JG (1995). Synchronized oscillations in interneuron networks driven by metabotropic glutamate receptor activation. *Nature* **373**, 612–615.

Wingrove PB, Wafford KA, Bain CJ & Whiting PJ (1994). The modulatory action of loreclezole at the γ-aminobutyric acid type A receptor is determined by a single amino acid in the β_2 and β_3 subunit. *Proc Natl Acad Sci U S A* **91**, 4569–4573.

Wisden W, Laurie DJ, Monyer H & Seeburg PH (1992). The distribution of 13 $GABA_A$ receptor subunit mRNAs in the rat brain. I. Telencephalon, diencephalon, mesencephalon. *J Neurosci* **12**, 1040–1062.

Xiang Z, Huguenard JR & Prince DA (1998). $GABA_A$ receptor-mediated currents in interneurons and pyramidal cells of rat visual cortex. *J Physiol* **506**, 715–730.

Yen CT, Conley M, Hendry SHC & Jones EG (1985). The morphology of physiologically identified GABAergic neurons in the somatic sensory part of the thalamic reticular nucleus in the cat. *J Neurosci* **5**, 2254–2268.

Ymer S, Schofield PR, Draguhn A, Werner P, Köhler M & Seeburg PH (1989). $GABA_A$ receptor β subunit heterogeneity: functional expression of cloned cDNAs. *EMBO J* **8**, 1665–1670.

Zhang SJ, Huguenard JR & Prince DA (1997). $GABA_A$ receptor-mediated currents in rat thalamic reticular and relay neurons. *J Neurophysiol* **78**, 2280–2286.

Acknowledgements

The authors thank Matthew V. Jones for careful reading of a preliminary version of this manuscript. This study was supported by NIH grants NS0647, NS072280, NS34774, NS10768-01, and the Pimley Research Fund.

Author's present address

M. M. Huntsman: Department of Pharmacology, Georgetown University, Washington, DC 20057, USA.